CONTRIBUTION FROM THE LAMP METALS AND COMPONENTS DEPARTMENT,
GENERAL ELECTRIC COMPANY, CLEVELAND, OHIO

Synthesis of Rare Earth Antimonate Pyrochlores and Cathodoluminescence of Europium(3+) in $3Gd_2O_3 \cdot Sb_2O_5$

BY D. K. NATH

Received December 29, 1969

A series of new pyrochlore compounds with the general formula $3Ln_2O_3 \cdot Sb_2O_5$ (where Ln = Nd, Sm, Eu, Gd, Tb, Dy, Ho, Er, Tm, or Yb) was prepared. The corresponding antimonates of La and Pr showed the formation of distorted pyrochlore. The lattice constants of the pyrochlore compounds were determined. Typical Eu^{3+} red and Tb^{3+} green emissions were observed in $3La_2O_3 \cdot Sb_2O_5$, $3Gd_2O_3 \cdot Sb_2O_5$, and $3Y_2O_3 \cdot Sb_2O_5$ as host crystals. The cathode ray excited Eu^{3+} spectrum in $3Gd_2O_3 \cdot Sb_2O_5$ as a host lattice was explained in the light of crystal field symmetry. The compound $3Gd_2O_3 \cdot Sb_2O_5$ showed a slight local distortion of the site symmetry D_{3d}.

I. Introduction

Compounds[1-3] isostructural with pyrochlore were paid much attention in the recent years after the discovery by Cook and Jaffé[4] that $Cd_2Nb_2O_7$ is ferroelectric at certain temperatures. The mineral pyrochlore[5] has the average composition $NaCa(NbTa)O_6(F,OH)$ which can be generally formulated as $A_2B_2X_7$. The space group[6] for pyrochlore is $Fd3m$-O_h^7 with $Z = 8$. The atomic arrangement in a unit cell of pyrochlore is as follows: 16 A in 16(c), 16 B in 16(d), 8 X_I in 8(a), and 48 X_{II} in 48(f).

Its structure type may be described as an ordered distorted fluorite, $A_2B_2X_7\square$ with one out of every eight anions missing.[3] The smaller B cations are highly charged and arranged in a continuous network of corner-sharing $(B_2X_6)_\infty$ octahedra. The larger A cations and the seventh anion occupy holes formed by the octahedral network in a way which leaves the larger cations surrounded by eight anions.

A large number of crystal chemical substitutions on A, B, and X sites of pyrochlore are possible.[7] This report is concerned with the synthesis and determination of the unit cell dimensions of a series of rare earth antimonates (Ln_2LnSbO_7) which are isostructural with pyrochlore. Typical Eu^{3+} red and Tb^{3+} green emissions were observed with cathode ray excited $3Ln_2O_3 \cdot Sb_2O_5$ where Ln = La, Gd, or Y. The reflectance and emission spectra of Eu^{3+} red emission have been discussed.

II. Experimental Section

Ln_2O_3 (where Ln = La, Pr, Nd, Sm, Eu, Gd, Tb, Dy, Ho, Er, Tm, or Yb) of 99.9% purity and AR grade Sb_2O_3 in a molar ratio of 1:1 were mixed intimately under acetone in an agate mortar. The samples were prepared by heating the dried oxide mixtures in covered Pt crucibles at 1000° for 16 hr followed by regrinding and reheating between 1350 and 1450° for a period of 65–78 hr. Heating up to 1450° was carried out in a Globar furnace. Still higher temperature (1650°) was obtained with a Lepel induction furnace.

The formation of the compounds $3Ln_2O_3 \cdot Sb_2O_5$ was detected by the weight change experiment and confirmed by chemical analyses. Most of these rare earth antimonates cannot be dissolved in HCl or H_2SO_4 or by the conventional fusion methods using Na_2CO_3 or NaOH or $K_2S_2O_7$. A special method was developed to dissolve $3Ln_2O_3 \cdot Sb_2O_5$ compounds. This method consists in the reduction of Sb^{5+} to Sb^{3+} by passing SO_2 into a hot suspension of the powdered specimens in 50% H_2SO_4 for 1–8 hr. The suspension was diluted with water whenever fuming occurred. The heating was done on a magnetic hot plate until a clear solution was obtained. At the end SO_2 was purged by N_2 and the clear solution was titrated for antimony by 0.05 N $KBrO_3$ solution using methyl orange as an indicator. The rare earths were determined by EDTA using CuPAN as an indicator.

Phase analyses were made largely by the use of a GE XRD. Ni-filtered Cu Kα radiation and a perma quartz plate[8] as an external standard were used. The X-ray powder diffraction patterns were run at the highest sensitivities on the linear scale of the diffractometer to detect extremely weak reflections. The d spacings and relative intensities were obtained from the diffractometer traces at a scanning rate of 0.2°/min. The peak positions at high angles were determined from the α_1 and α_2 peaks by finding the midpoint of the line at 50% of their maximum intensities. The lattice constants were obtained from Nelson–Riley extrapolation.[9] Computer programs gave the calculated d values.

A Cary 14 spectrophotometer and a Model 1411 reflectance accessory specially modified by Dr. J. A. Marquisee of this laboratory were used to record emission spectra of the phosphors. The modified instrument records reflectance as well as photo-excited and electron-excited emission spectra. Samples to be examined under cathode ray were coated on quartz disks and placed in a small demountable cathode ray tube. Emitted light entered the Cary optical path *via* a first-surface mirror. The dispersed radiation was detected by a photomultiplier tube mounted on a sliding carriage in the high-intensity source compartment. The reflectance and cathode ray spectra were taken at room temperature.

III. Results and Discussion

1. Crystal Chemical Aspects.—The results on the chemical determination of the rare earth and Y antimonates are given in Table I.

The pyrochlore structure has two special extinction rules in addition to the ones present for face-centered cubic symmetry. (a) The anions at (a) and (f) sites will generate the reflections of the type $h + k + l =$

(1) S. Roth, *J. Res. Nat. Bur. Stand.*, **56**, 17 (1956).
(2) S. Marzullo and E. N. Bunting, *J. Amer. Ceram. Soc.*, **41**, 40 (1958).
(3) E. Aleshin and R. Roy, *ibid.*, **45**, 18 (1962).
(4) W. R. Cook, Jr., and H. Jaffé, *Phys. Rev.*, **88**, 1426 (1952).
(5) C. Palache, H. Berman, and C. Frondel, Dana's System of Mineralogy," Vol. 1, 7th ed, Wiley, New York, N. Y., 1944, pp 745–808.
(6) H. V. Gaertner, *Neues Jahrb. Mineral., Geol. Paleontol.*, **61**, 1 (1930).
(7) A. Ferrari and L. Cavalca, *Gazz. Chim. Ital.*, **74**, 117 (1944).
(8) Perma quartz, X-Ray Powder Data File, Card No. 5-0490, ASTM, (1960).
(9) L. V. Azaroff and M. J. Buerger, "The Powder Method in X-Ray Crystallography," McGraw-Hill, New York, N. Y., 1958, p 342.

$2n + 1$ or $4n$. (b) The cations at (c) and (d) sites will generate the reflections of the types $h = 2n + 1$ or $4n + 2$ or $4n$, $k = 2n + 1$ or $4n + 2$ or $4n$, and $l = 2n + 1$ or $4n + 2$ or $4n$.

The pyrochlore structure has its own characteristic diffraction pattern which is different from those of the closely related structures, *e.g.*, fluorite, weberite, thortveitite, and c-type rare earth oxides.

The X-ray powder data of $3Gd_2O_3 \cdot Sb_2O_5$ as a representative compound of the rare earth antimonate pyrochlore group are given in Table II. The lattice constants and densities are given in Table III.

TABLE I

CHEMICAL ANALYSES OF THE RARE EARTH AND Y ANTIMONATES

	Theoret %		Obsd %	
	Ln_2O_3	Sb_2O_5	Ln_2O_3	Sb_2O_5
$3La_2O_3 \cdot Sb_2O_5$	75.13	24.89	74.89	24.76
$3Pr_2O_3 \cdot Sb_2O_5$	75.36	24.64	75.14	24.80
$3Nd_2O_3 \cdot Sb_2O_5$	75.73	24.27	75.56	24.39
$3Sm_2O_3 \cdot Sb_2O_5$	76.38	23.62	76.23	23.51
$3Eu_2O_3 \cdot Sb_2O_5$	76.55	23.45	76.39	23.29
$3Gd_2O_3 \cdot Sb_2O_5$	77.07	22.93	76.92	22.70
$3Tb_2O_3 \cdot Sb_2O_5$	77.24	22.76	77.12	22.62
$3Dy_2O_3 \cdot Sb_2O_5$	77.57	22.43	77.39	22.31
$3Ho_2O_3 \cdot Sb_2O_5$	77.80	22.20	77.68	22.09
$3Er_2O_3 \cdot Sb_2O_5$	78.01	21.99	77.85	21.82
$3Tm_2O_3 \cdot Sb_2O_5$	78.16	21.84	78.02	21.70
$3Yb_2O_3 \cdot Sb_2O_5$	78.51	21.49	78.39	21.37
$3Y_2O_3 \cdot Sb_2O_5$	67.68	32.32	67.46	32.60

TABLE II

X-RAY POWDER DIFFRACTION DATA FOR $3Gd_2O_3 \cdot Sb_2O_5$, $3La_2O_3 \cdot Sb_2O_5$, AND $3Pr_2O_3 \cdot Sb_2O_5$[a]

	$3Gd_2O_3 \cdot Sb_2O_5$ (P)			$3La_2O_3 \cdot Sb_2O_5$ (DP)		$3Pr_2O_3 \cdot Sb_2O_5$ (DP)		$3La_2O_3 \cdot Sb_2O_5$ (U)	
hkl	d_{obsd}, Å	d_{calcd}, Å	I/I_0	*d*, Å	I/I_0	*d*, Å	I/I_0	*d*, Å	*I*
222	3.07	3.07	100	3.40	9	3.37	8	3.68	w
400	2.666	2.666	35	3.16	81	3.14	86	3.58	s
440	1.880	1.882	39	3.13	100	3.10	100	3.48	s
622	1.605	1.605	31	3.05	6	3.02	6	3.22	m
444	1.536	1.536	7	2.896	11	2.87	9	2.858	m
800	1.330	1.330	5	2.770	18	2.736	25	2.697	s
662	1.220	1.221	9	2.700	34	2.680	41	2.523	m
840	1.189	1.190	4	2.669	6	...	...	2.477	w
844	1.087	1.087	4	2.460	3	2.443	3	2.382	w
666	1.024	1.024	4	2.376	3	2.356	4	2.356	w
10,2,2				2.150	5	2.118	7	2.286	w
				2.130	5	...	...	2.242	w
				2.089	4	2.067	3	2.174	w
				2.053	5	2.027	8	2.134	m
				2.034	2	2.017	5	2.041	w
				1.988	4	1.969	3	1.987	w
				1.935	42	1.916	44	1.969	m
				1.901	5	1.879	4	1.888	w
				1.866	3	1.844	2	1.847	m
				1.843	4	1.826	6	1.772	w
				1.751	7	1.731	8	1.691	w
				1.667	15	1.644	14		
				1.643	22	1.629	20		
				1.630	15				
				1.584	6				
				1.570	4				

[a] Abbreviations: DP, distorted pyrochlore; U, unknown structure; P, pyrochlore; w, weak; m, medium; s, strong.

The lanthanide contraction is shown in Figure 1 by plotting the lattice constant as a function of the radii of trivalent rare earth ions. It is expected from Figure 1 that a complete solid miscibility and a Vegard's law relationship may exist between the different members of the pyrochlore type rare earth antimonates.

TABLE III

LATTICE CONSTANT AND DENSITY OF THE RARE EARTH AND Y ANTIMONATE PYROCHLORE COMPOUNDS

Compound	Lattice constant, Å	$D_{X\text{-ray}}$, g/cm³	D_{pycno}, g/cm³
$3Yb_2O_3 \cdot Sb_2O_5$	10.368	8.97	8.95
$3Tm_2O_3 \cdot Sb_2O_5$	10.410	8.74	8.72
$3Er_2O_3 \cdot Sb_2O_5$	10.448	8.56	8.51
$3Ho_2O_3 \cdot Sb_2O_5$	10.495	8.37	8.34
$3Dy_2O_3 \cdot Sb_2O_5$	10.522	8.22	8.20
$3Tb_2O_3 \cdot Sb_2O_5$	10.550	8.05	8.01
$3Gd_2O_3 \cdot Sb_2O_5$	10.638	7.77	7.73
$3Eu_2O_3 \cdot Sb_2O_5$	10.668	7.55	7.53
$3Sm_2O_3 \cdot Sb_2O_5$	10.720	7.39	7.37
$3Nd_2O_3 \cdot Sb_2O_5$	10.820	6.98	6.95
$3Y_2O_3 \cdot Sb_2O_5$	10.487	5.76	5.75

The X-ray patterns for $3Pr_2O_3 \cdot Sb_2O_5$ and $3La_2O_3 \cdot Sb_2O_5$ showed no pyrochlore formation. Among the two structural varieties identified in this group, the low-temperature form was converted completely to the other type by heating at 1400° for 60 hr at 1450° for 78 hr in the cases of the antimonates of Pr and La, respectively. These two types of structures are different from weberite (Na_2MgAlF_7) and thortveitite ($Sc_2Si_2O_7$) which are $A_2B_2X_7$ type compounds. The X-ray powder data on the two forms of lanthanum antimonate and the high-temperature form of praseodymium antimonate are given in Table I. The intensity normalized to 1 (222) and split-up *d* spacings of the "metals-only" reflections of the high-temperature form of these antimonates indicate a highly distorted pyrochlore structure. These structures were not indexed. On heating, $3Pr_2O_3 \cdot Sb_2O_5$ decomposed to $PrO_{1.83}$ at 1650° approximately.

2. Spectral Studies.—The fluorescence spectra of Eu-activated $3Gd_2O_3 \cdot Sb_2O_5$ under cathode ray excitation were run between 7000 and 3200 Å. The spectra are presented in Figure 2 in the range 6400–5700 Å because no transition could be observed in the other portions of the spectra. The band positions and assignments of the spectrum of $3Gd_2O_3 \cdot Sb_2O_5$(3.5% Eu) are given in Table IV. The reflectance spectrum is plotted in Figure 3.

TABLE IV

CATHODE RAY EXCITED SPECTRUM OF $3Gd_2O_3 \cdot Sb_2O_5$(3.5% Eu)

Transitions		No. of allowed CF[a] transitions	Obsd freq, cm^{-1}
From	To		
$^5D_1$ (A_{2g}) (E_g)	$^7F_3$ (A_{1g}) ($2A_{2g}$) ($2E_g$)	f[b]	17,292, 17,271, 17,094
$^5D_0$ (A_{1g})	$^7F_1$ (A_{2g}) (E_g)	2	17,020 16,978
$^5D_2$ (A_{1g}) ($2E_g$)	$^7F_6$ ($3A_{1g}$) ($2A_{2g}$) ($4E_g$)	f	16,807, 16,639, 16,507, 16,460
$^5D_0$ (A_{2g}) (E_g)	$^7F_2$ ($2A_{1g}$) ($2E_g$)	f	16,260
$^5D_1$ (A_{2g}) (E_g)	$^7F_4$ ($2A_{1g}$) (A_{2g}) ($3E_g$)	f	15,971

[a] Crystal field. [b] Forbidden.

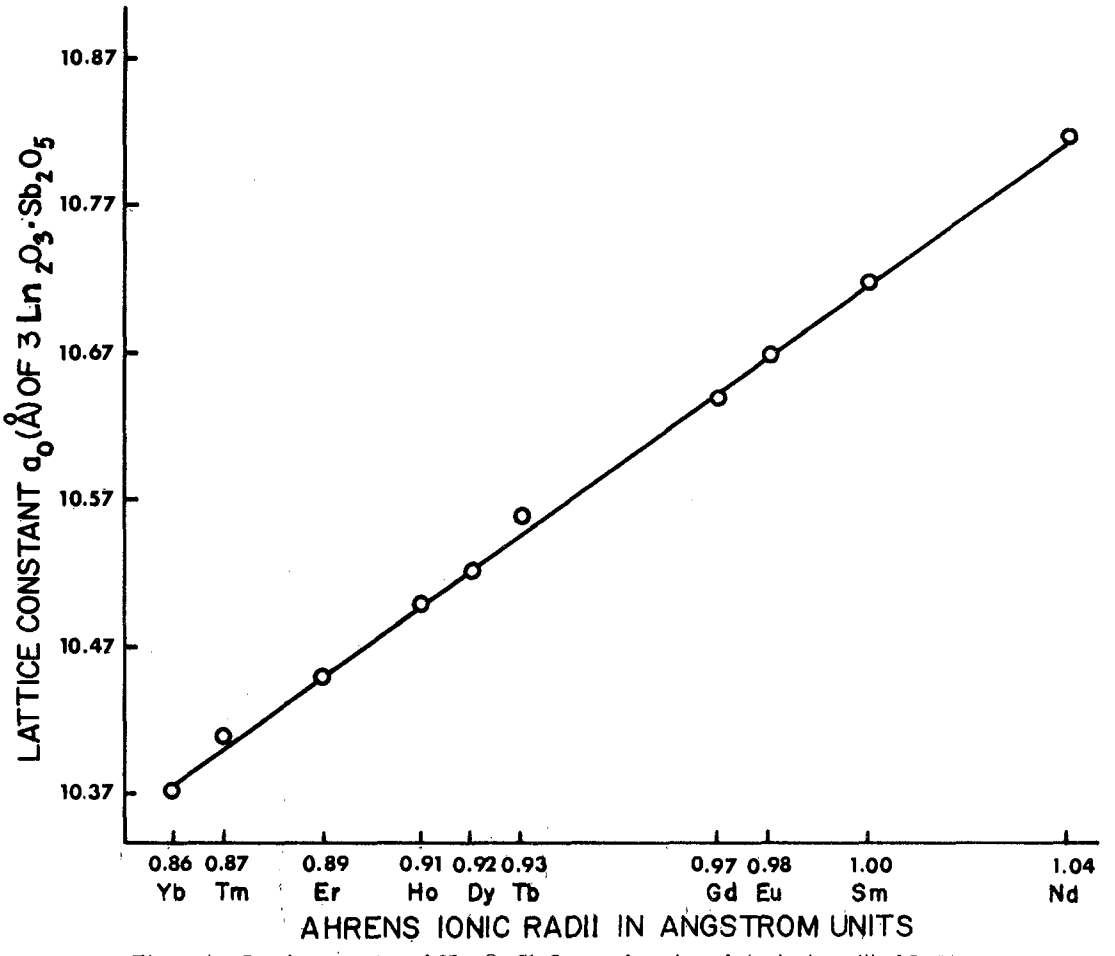

Figure 1.—Lattice constant of $3Ln_2O_3 \cdot Sb_2O_5$ as a function of the ionic radii of Ln^{3+}.

The crystallographic site symmetry at A and B atomic positions of pyrochlore ($A_2B_2X_7$) is D_{3d}. The identification of the observed transitions from ^5D_J multiplet to the ground-level ^7F_J terms of Eu^{3+} ($4f^6$) under cathode ray excitation was done on the basis of the electromagnetic selection rules and radiative probabilities which were widely discussed by several authors.[10,11] According to the Russell–Saunders scheme, the selection rules are: magnetic dipole: $\Delta S = \Delta L = 0$, $\Delta J = 0, \pm 1$ ($0 \not\leftrightarrow 0$); electric dipole; $\Delta S = 0$, $\Delta l = \pm 1$, $|\Delta L|$, $|\Delta J| \leq 2l$; electric quadrupole: $\Delta S = 0$, $|\Delta L|$, $|\Delta J| \leq 2$ ($0 \not\leftrightarrow 0$, $0 \not\leftrightarrow 1$).

Electric dipole transitions for intra f^n configurations are the result of the coupling of states of opposite parity by way of the odd terms of the crystal field expansion. The presence of a center of inversion in a crystalline symmetry, *e.g.*, D_{3d} will obviously forbid odd harmonics of the crystal field and hence electric dipole transitions. Magnetic and electric quadrupole transitions are parity allowed between levels of f^n configuration. The intensities of electric quadrupole transitions are extremely weak.[12,13] The net result is that the observed spectrum of Eu^{3+}-activated $3Gd_2O_3 \cdot Sb_2O_5$ will show magnetic dipole transitions predominantly. The probabilities for spontaneous emission of the most intense magnetic dipole transition will be due to $^5D_0 \rightarrow {}^7F_1$. In addition to the selection rules and spontaneous emission probabilities, the number of Stark splittings among the various levels was also considered to identify the observed transitions. The Γ_j representations and corresponding terms are given in Table V.

TABLE V
CRYSTAL FIELD SPLITTING OF TERMS OF $4f^6$ CONFIGURATION IN D_{3d} SITE SYMMETRY[a]

$\Gamma_0 \rightarrow A_{1g}$	$\Gamma_4 \rightarrow 2A_{1g} + A_{2g} + 3E_g$
$\Gamma_1 \rightarrow A_{2g} + E_g$	$\Gamma_5 \rightarrow A_{1g} + 2A_{2g} + 4E_g$
$\Gamma_2 \rightarrow A_{1g} + 2E_g$	$\Gamma_6 \rightarrow 3A_{1g} + 2A_{2g} + 4E_g$
$\Gamma_3 \rightarrow A_{1g} + 2A_{2g} + 2E_g$	

[a] The transition between two energy levels E_σ and E_ρ corresponding to the wave functions ψ_σ and ψ_ρ will be forbidden when $\int \psi_\sigma F_\lambda \psi_\rho \, d\tau = 0$. ψ_σ, F_λ, and ψ_ρ are functions from spaces whose bases generate the IRs Γ_σ, Γ_λ, and Γ_ρ. Since in D_{3d} symmetry, $\Gamma_\lambda = E_u$ and $\Gamma_\rho = E_u$, the only possible nonvanishing integrals are those in which $\Gamma_\sigma = A_{1g}, A_{2g}, E_g$.

The cathode ray excited spectra of $3Gd_2O_3 \cdot Sb_2O_5$ containing 2.5 and 3.5 mol % of Eu^{3+} in the Gd^{3+} site showed the same features. The most intense bands in the spectra were identified as the transition $^5D_1 \rightarrow {}^7F_3$ at 17,292, 17,271, and 17,094 cm^{-1}. The appearance of this forbidden electric dipole transition as the

(10) C. Brecher, H. Samelson, and A. Lempicki, "Optical Properties of Ions in Crystals, Conference at the Johns Hopkins University, Baltimore, Md., Sept 12–14, 1966," Interscience, New York, N. Y., 1966, pp 73–83.

(11) J. J. Weber, ref 10, pp 467–483.

(12) L. J. F. Broer, C. J. Gorter, and J. Hoogschagen, *Physica*, **11**, 231 (1945).

(13) M. A. El'yashevich, "Spectra of the Rare Earths," Atomic Energy Commission Translation No. 4403, Department of Commerce, Washington, D. C., 1961.

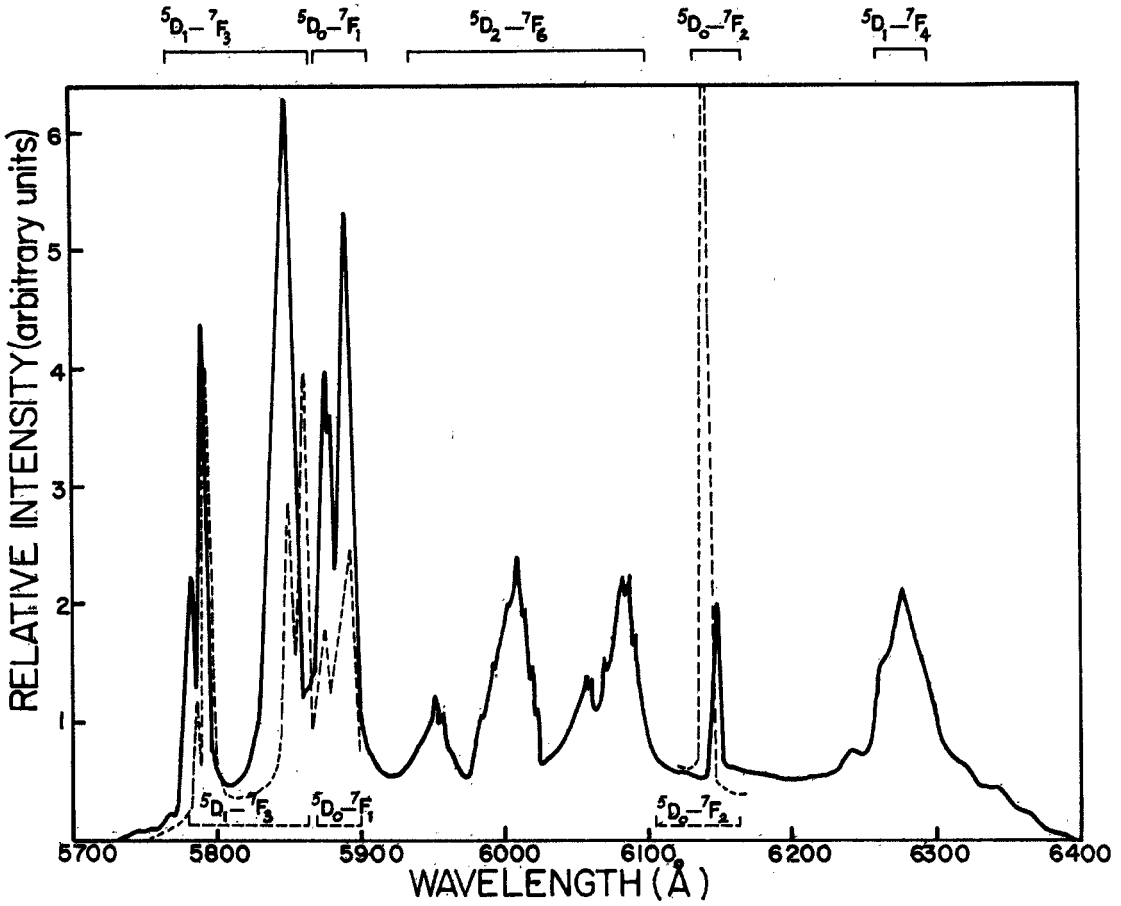

Figure 2.—Cathode ray excited spectra of $3Gd_2O_3 \cdot Sb_2O_5$(3.5% Eu) (solid line) and $3Gd_2O_3 \cdot Sb_2O_5$(3.5% Eu) fluxed by $KSbO_3$ (dashed line).

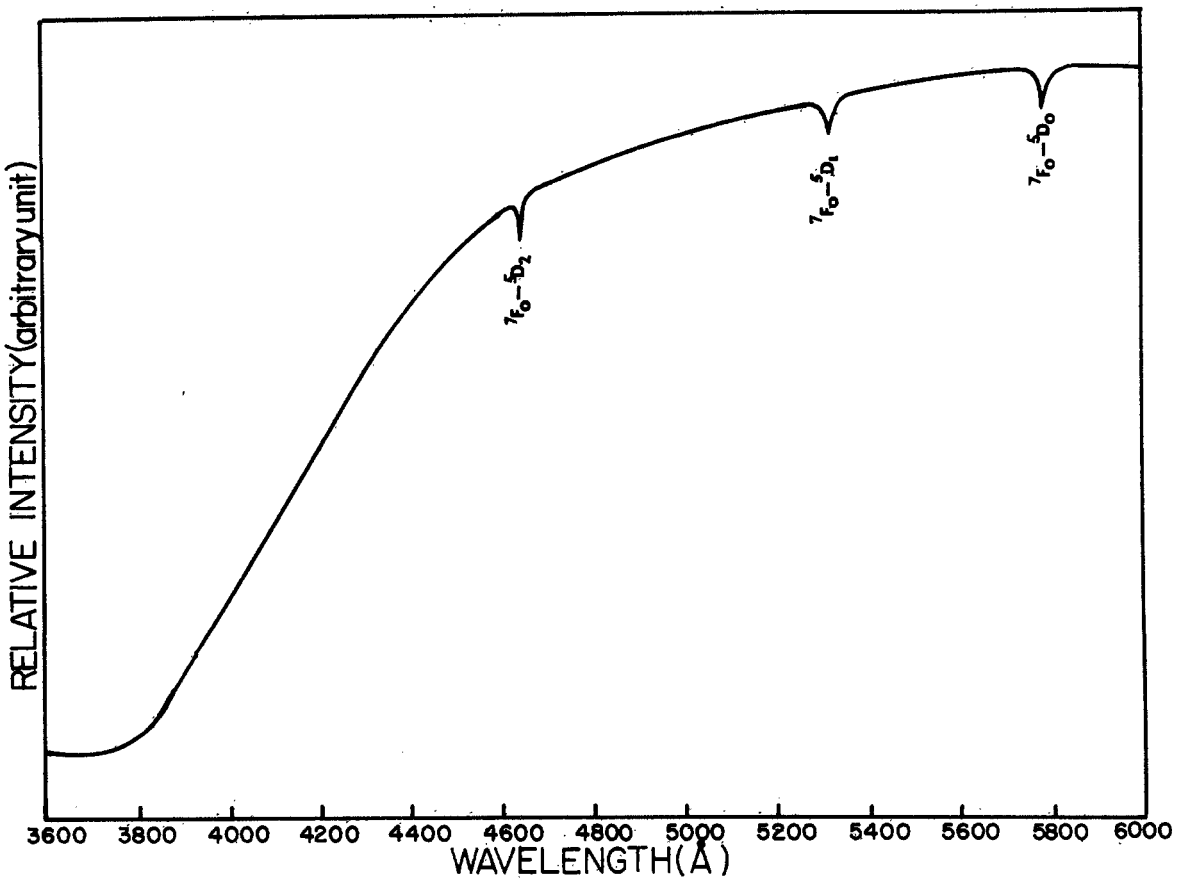

Figure 3.—Reflectance spectrum of $3Gd_2O_3 \cdot Sb_2O_5$(3.5% Eu).

most intense band in the spectra indicates that a strict center of inversion is destroyed in the site symmetry. The presence of the rare earth ions in the B site of the pyrochlore ($A_2B_2X_7$) structure in Gd_2GdSbO_7 creates a local distortion due to the considerable difference in the ionic radii of Gd^{3+} (0.97 Å) and Sb^{5+} (0.62 Å). The rare earth ion at the A site is coordinated to a regular framework of oxygen octahedra and two other oxygen atoms linearly at a shorter distance. The lowering of site symmetry at the B site will cause a distortion of the (GdO_8) polyhedra at the A site. Although the degree of distortion may be negligibly small to retain the basic pyrochlore structure, the highly sensitive Eu^{3+} emissions will respond to such a deviation from the strict center of symmetry. Blasse, *et al.*,[14] observed the same kind of phenomenon in the fluorescence spectrum of $LaTiSbO_6$–Eu (site symmetry, D_{3d}) where the forbidden electric dipole transition $^5D_0 \rightarrow {}^7F_2$ was found to be stronger than the magnetic dipole transition $^5D_0 \rightarrow {}^7F_1$.

The transition $^5D_0 \rightarrow {}^7F_1$ split up into two crystal field components at 17,020 and 16,978 cm^{-1} corresponding to a nondegenerate (A_{2g}) and a doubly degenerate (E_g) level as expected for D_{3d} symmetry. The intensity of these bands was very similar to that of the transition $^5D_1 \rightarrow {}^7F_3$.

Four well-resolved band areas at 16,807, 16,639, 16,507, and 16,460 cm^{-1} could be observed for the transition $^5D_2 \rightarrow {}^7F_6$. The broken nature of the bands indicates mixing of the closely situated other crystal field components. The transition $^5D_0 \rightarrow {}^7F_2$ appeared as a narrow band at 16,260 cm^{-1} and did not show any crystal field splitting. The weak intensity of this band suggests that the distorted site symmetry will be very close to D_{3d}.

The weak band at 15,971 cm^{-1} was assigned to the transition $^5D_1 \rightarrow {}^7F_4$. The broad weak band at 16,026 cm^{-1} was most probably due to the noncentrosymmetric vibrational modes of the surroundings of the rare earth ion. Weber and Schaufele[15] reported this kind of transition with $SrTiO_3$–Eu.

The reflectance spectrum (Figure 3) showed three weak and sharp bands at 17,256, 18,774, and 21,523 cm^{-1} corresponding to the transitions $^7F_0 \rightarrow {}^5D_0$, $^7F_0 \rightarrow {}^5D_1$, and $^7F_0 \rightarrow {}^5D_2$, respectively.

The effect of distortion of the D_{3d} site on the cathode ray spectra of $3Gd_2O_3 \cdot Sb_2O_5$(3.5% Eu) was further studied by fluxing with $KSbO_3$ which has a pyrochlore structure. A mixture of $3Gd_2O_3 \cdot Sb_2O_5$(3.5% Eu)–$KSbO_3$ in a molar ratio of 1:1 was heated in air at 1300° for 16 hr. The sample was washed in boiling water. The X-ray diffraction pattern of this sample showed a single phase $3Gd_2O_3 \cdot Sb_2O_5$ with a slight change in the d values suggesting a solid solution. The cathode ray spectrum of this sample (Figure 2) showed the electric dipole transition $^5D_0 \rightarrow {}^7F_2$ and $^5D_1 \rightarrow {}^7F_3$ to be the strongest ones although the magnetic dipole transition $^5D_0 \rightarrow {}^7F_1$ appeared as a pair of fairly weak bands. Obviously the presence of large K^+ (1.33 Å) ions in the lattice of $3Gd_2O_3 \cdot Sb_2O_5$ caused further distortion of D_{3d} site symmetry.

Acknowledgment.—The author is indebted to Miss J. Cooper of Lighting Research Laboratory for the computer program on the cubic crystal structure, Dr. J. Marquisee of this laboratory for running the spectra, and Mr. J. Hunter of this laboratory for the chemical analyses. The author is also thankful to Drs. T. Soules and R. Hickok of Lighting Research Laboratory and Messrs. R. McCauley of the Pennsylvania State University and S. Jones of this laboratory for their helpful discussions.

(14) G. Blasse, A. Bril and W. C. Nieuwpoort, *J. Phys. Chem. Solids*, **27**, 1587 (1966).

(15) M. J. Weber and R. F. Schaufele, *Phys. Rev.*, **138**, 1544A (1965).

CONTRIBUTION FROM THE CHEMISTRY DEPARTMENT,
UNIVERSITY OF UTAH, SALT LAKE CITY, UTAH 84112

A Fluorine-19 Nuclear Magnetic Resonance Study of Tin Tetrafluoride Diadducts of Various Aromatic Amine Oxides

BY C. E. MICHELSON[1] AND RONALD O. RAGSDALE*

Received April 2, 1970

An ^{19}F nmr study of diadducts of SnF_4 with 19 aromatic amine oxides is reported. The results indicate that the steric nature of the ligand is probably more important than the base strength in determining the relative chemical shifts. The trans isomer is identified in all of the complexes whereas the cis isomer is present only with the less bulky ligands.

Introduction

The donor properties of various aromatic amine oxide systems have been reviewed recently.[2,3] It has been shown that in most cases there is a linear correlation between some observable property such as an infrared stretching frequency or a ^{19}F chemical shift and a suit-

* To whom correspondence should be addressed.

(1) NDEA Title IV Predoctoral fellow, 1966–1969. This paper is a portion of the Ph.D. thesis of C. E. Michelson to be submitted to the Chemistry Department of the University of Utah.

(2) M. Orchin and P. J. Schmidt, *Coord. Chem. Rev.*, **3**, 345 (1968).

(3) R. G. Garvey, J. H. Nelson, and R. O. Ragsdale, *ibid.*, **3**, 375 (1968).